

## Isotropic-nematic interface of soft spherocylinders

Muataz S. Al-Barwani\* and Michael P. Allen

*H.H. Wills Physics Laboratory, University of Bristol, Royal Fort, Tyndall Avenue, Bristol BS8 1TL, United Kingdom*

(Received 13 June 2000)

The isotropic-nematic interface of a simple model of liquid-crystal molecules has been investigated using computer simulation, and by numerical minimization of the Onsager free-energy functional. The molecules are represented by long spherocylindrical particles interacting via the Kihara potential. The agreement between simulation and theory is excellent, apart from the bulk coexistence densities which are over estimated by the theory. Planar alignment of the molecules at the interface is preferred in all cases. The number density profile is found to vary monotonically, both in simulation and in theory. Biaxiality of the molecular orientational distribution near the interface is demonstrated.

PACS number(s): 61.30.Cz, 61.20.Ja, 68.10.-m, 07.05.Tp

### I. INTRODUCTION

In 1949 Onsager demonstrated that a system of long rigid rodlike molecules, interacting with each other through steric excluded-volume interactions, exhibits a first-order isotropic ( $I$ ) to nematic ( $N$ ) phase transition at sufficiently high density [1]. When the nematic and isotropic phases coexist, the interface breaks both translational and orientational symmetry. Though the bulk free energy of the nematic phase is independent of the orientation direction, the director  $\mathbf{n}$ , the surface tension does depend on  $\mathbf{n}$ . In the absence of other effects, the system will adopt the orientation for which the surface tension is minimized [2]. This effect of the interface on molecular alignment is called *anchoring*.

The isotropic-nematic interface is one of the simplest interfaces, since for all practical purposes the isotropic and nematic liquids are incompressible, so the pressure is not an important experimental parameter. Furthermore, due to the small difference between the isotropic and nematic densities at the transition, the density is not believed to play an important role in determining the interfacial properties [3]. An understanding of the interfacial alignment in this system presents some fundamental questions about which molecular features, if any, are necessary to produce a certain type of anchoring. Nonetheless, there are very few investigations using computer simulations to try and understand the behavior of the  $I$ - $N$  interface. This is perhaps because, for molecular thermotropic liquid crystals, the phase transition is only weakly first order, and fluctuations play a dominant role.

As with the nematic-vapor interface, the  $I$ - $N$  interface shows a different anchoring alignment for different types of liquid crystals. Experiments show that the molecule MBBA prefers planar anchoring [4] while some members of the cyanobiphenyl ( $n$ CB) series prefer oblique anchoring [5]. This seems to indicate that long-range electrostatic interactions might be the driving force behind oblique anchoring, since the  $n$ CB series have strong dipoles. No homeotropic anchoring (i.e., normal to the  $I$ - $N$  interface) has been observed experimentally.

Most theoretical studies of the  $I$ - $N$  interface [6–12] predict planar anchoring. An exception is the work of Hołyst and Poniewierski [2] which predicts oblique anchoring. Much of this work uses the Onsager expression for the free energy, which becomes valid in the limit of very high elongation. Computer simulations of the  $N$ - $I$  interface for moderately elongated particles (length/width=3) [13] indicate that planar alignment is favored; however, this system was stabilized by maintaining a temperature difference between the two phases, and is consequently not at thermodynamic equilibrium. Recently, Allen [14] investigated the  $I$ - $N$  interface for highly elongated ellipsoidal molecules (length/width =15) at equilibrium, using parallel confining walls to control the molecular alignment in the nematic phase. Very good agreement was obtained between simulation results and Onsager theory predictions of the order parameter profile and the density profile across the interface. More recent simulation work has succeeded in calculating the surface tension for parallel and normal alignment, confirming that this system also exhibits planar anchoring [15].

In both the simulation and theory of Ref. [14], the number density profile for the planar alignment case was found to vary monotonically. This contrasts qualitatively with the theoretical study of Koch and Harlen [12], in which the infinite elongation limit was taken; this showed a significant minimum in this profile on the isotropic side of the interface. Part of the motivation for the current work is to extend both the simulations and the Onsager analysis to much longer particles, to discover whether the nonmonotonic profile appears.

The model used in this work is described in Sec. II, the theoretical approach is summarized in Sec. III, details of the simulations are presented in Sec. IV, the results are given in Sec. V, and we summarize our conclusions in Sec. VI.

### II. MODEL

The particles used in this study interact as purely repulsive soft spherocylinders of elongation  $L$  and diameter  $D$ . Specifically, the pair potential between particles 1 and 2 takes the form

$$v_{12} = 4 \epsilon_0 \left[ \left( \frac{D}{s_{12}} \right)^{12} - \left( \frac{D}{s_{12}} \right)^6 \right] + 1, \quad s_{12} \leq 2^{1/6} D \quad (1)$$

\*Present address: Physics Department, Sultan Qaboos University, P.O. Box 36, Al-Khod, Muscat 123, Oman.

and it is zero for  $s_{12} > 2^{1/6}D$ . Here,  $s_{12}$  is the minimum distance between two line segments of length  $L$ ; the potential increases rapidly as this distance falls below the diameter  $D$ . Thus, this potential is a good approximation to the hard spherocylinder model which has been extensively studied by simulation [16,17], but it is continuous and hence more convenient for use in molecular-dynamics simulation. The length to diameter ratios used in this work were  $L/D=20$  and  $L/D=50$ . In the simulations, we set  $D=1$ , defining a unit of length, and choose  $k_B T = \epsilon_0 = 1$ , defining both energy units and the temperature of this study. (For this model, the phase diagram is much less sensitive to temperature than analogous models having attractive potentials). The particle mass was chosen to be  $m=1$ . The moment of inertia was taken to be  $I = \frac{1}{4}mL^2$ , corresponding to two point masses ( $m/2$ ) situated at the ends of the line segment; thus, in reduced units,  $I/mD^2=100$  for  $L/D=20$  and  $I/mD^2=625$  for  $L/D=50$ .

In the asymptotic limit  $L/D \rightarrow \infty$ , Onsager theory predicts that the  $I$ - $N$  transition occurs at a number density  $\mathcal{O}(1/L^2D)$ ; therefore, it is convenient to quote number densities as the dimensionless combination  $\rho L^2D$ .

### III. ONSAGER THEORY

Theoretical calculations were done using Onsager's density-functional theory [1]. The construction and minimization of the Onsager free-energy functional followed closely the procedure described before [18,14]. The excess part of the Helmholtz free energy  $\mathcal{F} = \mathcal{F}^{\text{id}} + \mathcal{F}^{\text{ex}}$  is expressed in terms of the one-particle density  $\varrho^{(1)}(\mathbf{r}, \mathbf{u})$  where  $\mathbf{r} = (x, y, z)$  is the position vector and  $\mathbf{u}$  the unit vector defining the orientation:

$$\mathcal{F}^{\text{ex}}[\varrho^{(1)}] = -\frac{1}{2}k_B T \int d\mathbf{r}_1 \int d\mathbf{u}_1 \int d\mathbf{r}_2 \int d\mathbf{u}_2 \\ \times \varrho^{(1)}(\mathbf{r}_1, \mathbf{u}_1) \varrho^{(1)}(\mathbf{r}_2, \mathbf{u}_2) f(\mathbf{r}_{12}, \mathbf{u}_1, \mathbf{u}_2).$$

Here  $\mathbf{r}_{12} = \mathbf{r}_1 - \mathbf{r}_2$ , and  $f(\mathbf{r}_{12}, \mathbf{u}_1, \mathbf{u}_2) = \exp(-v_{12}/k_B T) - 1$ ; this is the leading term in a low-density virial expansion. Since  $\varrho^{(1)}$  is independent of  $x$  and  $y$ ,  $f$  may be integrated over these coordinates. The logarithm of the density is expanded in spherical harmonics, on a discrete grid in  $z$  with an interval  $\delta z = 0.01L$  in each case  $L/D = 20, 50$ :

$$\ln \varrho^{(1)}(z_i, \mathbf{u}) = \sum_{lm} C_{i;lm} Y_{lm}(\mathbf{u})$$

and with periodic boundary conditions in the  $z$  direction. In the current application, this expansion was taken to fourth order in the  $Y_{lm}(\mathbf{u})$  (restricting to second order was found to change the coexistence pressure and densities by  $\sim 1\%$ ). All relevant orientational integrals were expressed in terms of spherical-harmonic coefficients of the density up to order 10 (reducing to order 8 was found to change the coexistence pressure and densities by  $\sim 0.01\%$ ). The parameters  $C_{i;lm}$  were varied to minimize the grand potential  $\beta\Omega[\varrho^{(1)}] \equiv \beta\mathcal{F}[\varrho^{(1)}] - \beta\mu N$  of an  $I$ - $N$  film system at the coexistence value of the chemical potential  $\mu$ , determined by a preliminary bulk calculation. A total of 1750 grid points was em-

ployed in  $z$ , i.e., the box length was taken to be  $17.5L$  in each case, with approximately equal amounts occupied by each phase.

### IV. SIMULATIONS

The simulation study was divided in two parts: the location of the coexisting state points by Gibbs ensemble Monte Carlo (GEMC) and the simulation of a nematic film surrounded by a coexisting isotropic liquid, by molecular dynamics (MD). Both techniques are quite standard and described in detail elsewhere [19,20].

Initial isotropic and nematic configurations were prepared in almost cubic boxes with periodic boundary conditions: the box side was  $L \approx 50D$ , containing  $N \approx 1200$  particles for the  $L/D=20$  system, and  $L \approx 103D$ , containing  $N \approx 1800$  particles for  $L/D=50$ . As a guide to the initial densities, the coexistence values observed by Bolhuis and Frenkel [17] for hard spherocylinders were used. An overall density  $\rho L^2D = 3.55$  is well within the coexistence region for  $L/D=20$ , and  $\rho L^2D = 4.03$  similarly for  $L/D=50$ . An equilibration period of  $4 \times 10^4$  to  $6 \times 10^4$  sweeps was carried out using GEMC at constant temperature, total volume, and total number of particles. The number of particles exchanged between the two boxes was set to  $10^4$  particles attempted per sweep. In the volume-exchange moves, boxes (and particle coordinates) were only scaled in the  $z$  direction, keeping the  $x$  and  $y$  dimensions equal, so as to facilitate a later combination of the two phases.

To model the isotropic-nematic interface the phases have to be in spatial contact with each other. This was done by combining, end-to-end, four copies of the box containing the bulk nematic and four copies of the bulk isotropic phase, to form a nematic film surrounded by an isotropic fluid on both sides. These new boxes are fully periodic and have a total number of particles  $N=9600$  and  $N=14400$  for the  $L/D=20$  and the  $L/D=50$  cases, respectively. For the  $L/D=20$  system, two distinguishable anchoring orientations of the nematic director with respect to the interface were set up: the first parallel to the interface, the second normal to the interface. In addition, for  $L/D=20$ , further systems were set up, having double the transverse dimensions and containing  $N=38400$  particles. In the case of the  $L/D=50$  system, only the parallel orientation was studied. When combining the two phases as just described, molecular overlaps occur at the interfaces. Equilibration runs of  $\sim 10^3$  MC (Monte Carlo) sweeps were done using constant- $NVT$  Monte Carlo to eliminate overlapping molecules at the interfaces. Following this, molecular-dynamics simulations were employed.

The domain-decomposition parallel MD code GBMEGA [21] was modified to include the potential of Eq. (1) and the corresponding forces and torques. A time step  $\delta t = 0.01$  (in the reduced units defined in Sec. I) was found to give reasonably small energy fluctuations  $\sim \mathcal{O}(10^{-3})$ ; this time step is similar to that used by Grest and Kremer [22] for a bead-spring model that uses a comparable type of repulsive Lennard-Jones potential.

Equilibration and production runs were done at a constant temperature and constant volume. For the  $N=9600$ ,  $L/D=20$  system with the nematic director parallel to the interface, an equilibration period of  $1.2 \times 10^6$  MD steps was done

followed by a production period of  $1.5 \times 10^6$  steps during which configurations were stored every 500 time steps for later analysis of interfacial properties. The system with the director normal to the interface took  $1.3 \times 10^6$  equilibration steps and  $1.4 \times 10^6$  production steps. During the run, the system with the nematic director normal to the interface began to rotate towards a planar orientation: to prevent this, a director constraint method was applied [23]. For the  $L/D = 50$  case, an equilibration period of  $1.4 \times 10^6$  MD steps was done with a production period of  $1.7 \times 10^6$  steps. Slightly longer equilibration and production times were needed for the longer spherocylinders which rotated much more slowly than their shorter counterparts, this was because of their larger moment of inertia. The code was run on a Cray T3E using 32 processors. For the larger  $N = 38\,400$ ,  $L/D = 20$  systems, equilibration took  $1.9 \times 10^6$  steps and production took  $1.0 \times 10^6$  steps; these systems were run on 64 processors of the Cray T3E. Simulations of the smallest ( $N = 9600$ ) system with  $L/D = 20$  showed some indications of finite-size effects due to the limited transverse dimensions, and accordingly all results in this paper refer to the larger ( $N = 38\,400$ ) system.

## V. RESULTS

Profiles of number density  $\rho(z)$  and the second-rank orientational order tensor  $\mathbf{Q}(z)$ , taken along the  $z$  axis of the box, were calculated for all the systems. This latter quantity is a symmetric, traceless tensor, defined

$$Q_{\alpha\beta}(z) = \frac{1}{N_{\mathcal{R}}} \sum_{i \in \mathcal{R}} \frac{3}{2} \left( u_{i\alpha} u_{i\beta} - \frac{1}{3} \delta_{\alpha\beta} \right), \quad \alpha, \beta = x, y, z,$$

in terms of the orientation vectors  $\mathbf{u}_i$  of each molecule  $i$ , and the sum is over the  $N_{\mathcal{R}}$  particles lying in a thin slab region  $\mathcal{R}$  around position  $z$ . Diagonalization of this order tensor yields three eigenvalues,  $S$ ,  $-\frac{1}{2}(S - \alpha)$ ,  $-\frac{1}{2}(S + \alpha)$ , which are conveniently expressed in terms of the nematic order parameter  $S(z)$  and the biaxiality order parameter  $\alpha(z)$  [11].

The order parameter profiles in the vicinity of each interface were fitted to a hyperbolic tangent function of the following form:

$$S(z) = \frac{1}{2}(S_N + S_I) + \frac{1}{2}(S_N - S_I) \tanh\left(\frac{z - z_{NI}}{\delta_S}\right) \quad (2)$$

where  $S_N$  and  $S_I$  are the nematic and isotropic second-rank order parameter, respectively,  $\delta_S$  is the thickness of the interface, and  $z_{NI}$  is the interface position in the simulation box. Keeping in mind that the interface might move during the simulation, each entire run was split up into ten subruns. Since the film had two interfaces, the order parameter profile  $S(z)$  around each one, averaged over each subrun, was fitted independently to the above hyperbolic tangent function; then the fitted value of  $z_{NI}$  was used to shift *all* profiles (order tensor and number density) together such that the center of the  $S(z)$  profile lay at the origin  $z_{NI} = 0$ . Finally, an average of all the profiles was carried out.

Figures 1–3 show the simulation results and Onsager theory predictions for all the systems studied. The widths of the interfaces were determined from the fitting and are presented in Table I. The interfacial thickness  $\delta_S$  and  $\delta_\rho$  of both

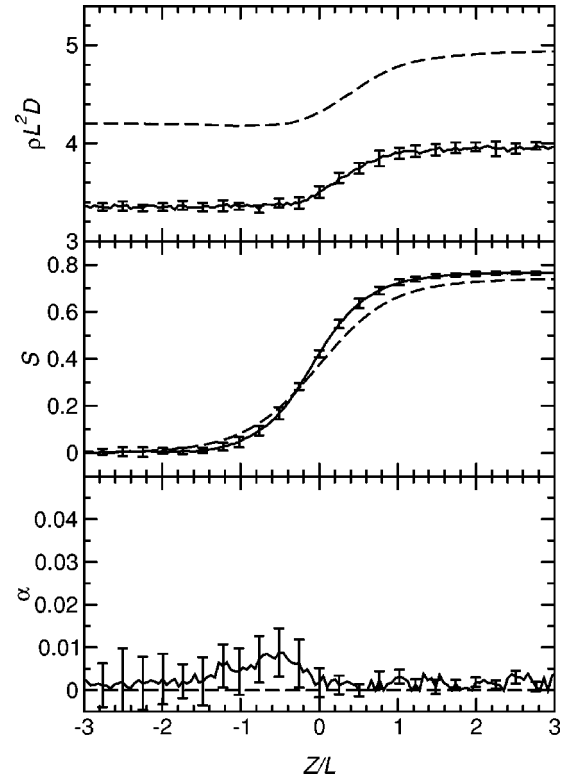


FIG. 1. Profiles for  $L/D = 20$  with the director aligned normal to the interface. We show the dimensionless number density  $\rho L^2 D$ , the nematic order parameter  $S$ , and the biaxiality parameter  $\alpha$  as functions of the dimensionless position  $z/L$ . Simulation results are shown as solid lines with some indicative error bars; Onsager theory predictions are shown as dashed lines. The origin  $z = 0$  is defined by the midpoint of the order parameter interface.

order and density profiles are  $\mathcal{O}(L/2)$  when the director is in the interface plane; the order parameter interface is slightly wider for normal alignment. This is in agreement with the work of Chen and Noolandi [10]. The width of the interface varies with the director angle in agreement with the findings of Allen [14] in his study of the isotropic-nematic interface of hard ellipsoids of revolution. In all cases, the positions of the order and density profiles do not coincide: the density interface lies to the nematic side of the order interface by about  $\mathcal{O}(L/3)$  in agreement with the findings of Allen [14]. The Onsager theory reproduces the observed profiles quite accurately, except that the bulk coexistence densities are overestimated. The widths and shifts are all slightly overestimated by the theory.

The number density profile for all these cases varies monotonically with  $z$ . This is in contrast to the Onsager theory predictions of Koch and Harlen [12], where a significant minimum was predicted for the case of in-plane alignment. We have attempted to reproduce such nonmonotonic profiles within the Onsager theory by minimizing the free energy from an appropriately perturbed starting configuration: in all cases, the free energy was reduced by smoothing out the perturbation and converging to the structures reported here. We should recall that the results of Ref. [12] were derived in the asymptotic limit  $L/D \rightarrow \infty$ , whereas the current results apply to  $L/D = 20$  and  $50$ . Nonetheless, these results strongly suggest that the profile will be monotonic even in the high elongation limit.

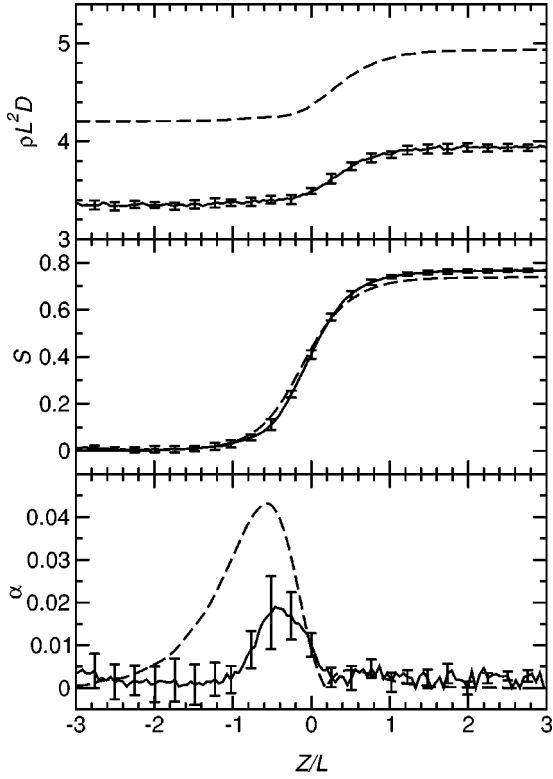


FIG. 2. Profiles for  $L/D=20$  with the director aligned in the plane of the interface. Notation is as for Fig. 1.

For in-plane director orientation, the interface removes the uniaxial symmetry of the bulk nematic phase [24,11]. Figure 3 shows that the biaxiality order parameter  $\alpha(z)$  is significantly nonzero (if small) in the interfacial region, in the case  $L/D=50$ . The agreement between simulation and theory is good: the observed effect is about 50% as large as the predicted effect, and the shape of the profile is very similar. The same can be seen in Fig. 2 for  $L/D=20$ , in-plane alignment, although here the simulation error bars are somewhat larger. Earlier attempts to measure this biaxiality effect [14] were hampered by finite statistics, which gave a small nonzero value of  $\alpha$  even in the isotropic phase; the current

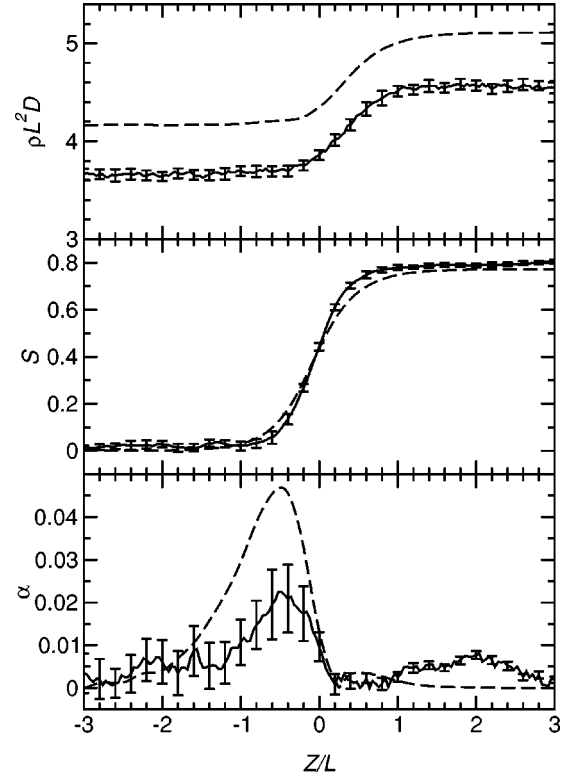


FIG. 3. Profiles for  $L/D=50$  with the director aligned in the plane of the interface. Notation is as for Fig. 1.

results do not suffer from this drawback, and they therefore constitute the first confirmation, by simulation, of the magnitude of this effect. In contrast, for normal alignment shown in Fig. 1, the theoretical prediction is zero by symmetry, and the simulation results are insignificant, within statistical errors.

## VI. CONCLUSIONS

A detailed simulation study of the isotropic-nematic coexistence and the interface region of a system of elongated soft spherocylinders has been carried out. The coexisting

TABLE I. Interface parameters from fitting profiles to a tanh function: simulation results (with error estimates in the last digit indicated in parentheses) and predictions of Onsager theory.  $S_I$  and  $S_N$  are, respectively, the isotropic and nematic order parameters, and  $\rho_I$  and  $\rho_N$  the corresponding number densities.  $\delta_S$  and  $\delta_\rho$  are the widths of the order parameter and number density interfaces, respectively, and  $\Delta$  is the difference in interface position between the two profiles.

	$L/D=20$		$L/D=50$	
	Simulation	Theory	Simulation	Theory
$S_I$	0.03(1)	0.00	0.06(1)	0.00
$S_N$	0.77(1)	0.74	0.81(1)	0.77
$\rho_I L^2 D$	3.35(1)	4.20	3.68(4)	4.17
$\rho_N L^2 D$	3.95(1)	4.93	4.57(4)	5.10
	Normal alignment		Planar alignment	
	Simulation	Theory	Simulation	Theory
$\delta_S/L$	0.7(1)	0.95	0.55(5)	0.61
$\delta_\rho/L$	0.6(2)	0.67	0.55(5)	0.60
$\Delta/L$	0.37(5)	0.53	0.37(4)	0.46
	Planar alignment		Planar alignment	
	Simulation	Theory	Simulation	Theory
$\delta_S/L$	0.42(6)	0.56	0.42(6)	0.56
$\delta_\rho/L$	0.4(1)	0.54	0.4(1)	0.54
$\Delta/L$	0.36(4)	0.44	0.36(4)	0.44

densities of the two phases were found for spherocylinders of elongation  $L/D=20$  and  $L/D=50$ . The two phases were then combined to form a nematic film surrounded by isotropic liquid. Interfaces were allowed to form where the two phases came into contact. It was observed that the molecules preferred an orientation that was parallel to the interface (planar anchoring) in agreement with experimental results for MBBA [4], with earlier theoretical predictions [10,12], and with simulations of related models [14,15]. We have compared our simulation results with a simple density-functional theory in the Onsager approximation, for exactly the same molecular models; this theory has no adjustable parameters. Good agreement between simulation and theory was obtained, apart from the well-known overestimation by theory of the precise coexistence densities. The interfacial profiles fitted well to a hyperbolic tangent function: no evidence was obtained, either in simulation or theory, of non-monotonic number density profiles [12]. The interface width was found to be of the order of half the molecular length, slightly more in the case of normal alignment. The positions of the orientational order interface and the density interface are displaced with respect to each other by about one-third of a molecular length. In all cases, Onsager theory slightly overestimates the interface widths and relative displacements, but the level of agreement is very good. Small, but significant, biaxiality effects were predicted for the case of

in-plane director alignment, as in previous theoretical studies [24,11]; we have succeeded in confirming this effect by computer simulation, and for the cases studied here it is, once more, overestimated by the theory.

Finally, we note that the current runs are not of sufficient length to determine accurately the surface tension of the  $I-N$  interface, which depends on the very small difference between normal and transverse stresses in the interfacial region. For the related hard-ellipsoid fluid, we have succeeded in carrying out measurements of this kind, and these results will be reported elsewhere [15].

#### ACKNOWLEDGMENTS

This research was supported by the EPSRC by providing computer time on the Cray T3E in Edinburgh through the High Performance Computing Initiative, and through support of local computing facilities. We would like to thank members of the Complex Fluids Consortium, whose program GBMEGA was used in this work, and G. Germano and K. Takeda for porting it to the Cray T3E and advising us on its use. M.S.A.B. would like to acknowledge support from Sultan Qaboos University. M.P.A. gratefully acknowledges helpful conversations with R. Evans, R. Roth, P. Tarazona, and R. van Roij concerning the Onsager calculations.

- 
- [1] L. Onsager, Ann. N.Y. Acad. Sci. **51**, 627 (1949).  
 [2] R. Holyst and A. Poniewierski, Phys. Rev. A **38**, 1527 (1988).  
 [3] M. Telo da Gama, in *Observation, Prediction and Simulation of Phase Transitions in Complex Fluids*, Vol. 460 of NATO Advanced Study Institute, Series C: Mathematical and Physical Sciences, edited by M. Baus, L. F. Rull, and J. P. Ryckaert (Kluwer Academic Publishers, Dordrecht, 1995), pp. 243–292 (Proceedings of the NATO Advanced Study Institute and Enrico Fermi Course LXXIX on “Observation and Prediction of Phase Transitions in Complex Fluids,” Varenna, Italy, 1994).  
 [4] D. Langevin and M. Bouchiat, Mol. Cryst. Liq. Cryst. **22**, 317 (1973).  
 [5] S. Faetti and V. Palleschi, Phys. Rev. A **30**, 3241 (1984).  
 [6] M. Doi and N. Kuzuu, Applied Polymer Symposia **41**, 65 (1985).  
 [7] H. Kimura and H. Nakano, J. Phys. Soc. Jpn. **55**, 4186 (1986).  
 [8] W. E. McMullen, Phys. Rev. A **38**, 6384 (1988).  
 [9] W. E. McMullen, Phys. Rev. A **40**, 2649 (1989).  
 [10] Z. Y. Chen and J. Noolandi, Phys. Rev. A **45**, 2389 (1992).  
 [11] S. M. Cui, O. Akcakir, and Z. Chen, Phys. Rev. E **51**, 4548 (1995).  
 [12] D. L. Koch and O. G. Harlen, Macromolecules **32**, 219 (1999).  
 [13] M. A. Bates and C. Zannoni, Chem. Phys. Lett. **280**, 40 (1997).  
 [14] M. P. Allen, J. Chem. Phys. **112**, 5447 (2000).  
 [15] A. J. McDonald, M. P. Allen, and F. Schmid (unpublished).  
 [16] S. C. McGrother, D. C. Williamson, and G. Jackson, J. Chem. Phys. **104**, 6755 (1996).  
 [17] P. Bolhuis and D. Frenkel, J. Chem. Phys. **106**, 666 (1997).  
 [18] M. P. Allen, Mol. Phys. **96**, 1391 (1999).  
 [19] M. P. Allen and D. J. Tildesley, *Computer Simulation of Liquids* (Clarendon Press, Oxford, 1989).  
 [20] D. Frenkel and B. Smit, *Understanding Molecular Simulation: From Algorithms to Applications* (Academic Press, San Diego, 1996).  
 [21] M. R. Wilson *et al.*, J. Comput. Chem. **18**, 478 (1997).  
 [22] G. S. Grest and K. Kremer, Phys. Rev. A **33**, 3628 (1986).  
 [23] M. P. Allen *et al.*, J. Chem. Phys. **105**, 2850 (1996).  
 [24] Z. Y. Chen, Phys. Rev. E **47**, 3765 (1993).